Control Systems Analysis of Antilock Braking System

Bethi Balagangadaran Kiran Sairam
Professor Nivii Kalavakonda Chandrasekar
Northeastern University
Boston, MA, USA
bethi.k@northeastern.edu

***Abstract*—This project presents the design, analysis, and implementation of an observer based state feedback controller for an automotive antilock braking system (ABS) using a quarter vehicle model. The analysis identifies an interesting equilibrium point at optimal slip ratio ($\lambda^* = 0.2$, $V_x^* = 20$ m/s), linearizes the nonlinear system dynamics at that point, and evaluates stability, controllability, and observability. The results show that the open loop system is unstable with two positive eigenvalues, fully controllable via braking torque, but not fully observable from slip measurements alone. The standard form decomposition shows that position is unobservable while velocity and slip dynamics are observable and sufficient for ABS control objectives. A pole placement state feedback controller is designed with settling time specification of 2 seconds and damping ratio 0.9, achieving regulation of slip ratio with 171% overshoot on the linearized plant. A Luenberger observer with poles five times faster than the controller converges within 0.446 seconds. The combined observer based controller shows performance nearly identical to perfect state feedback on the linear plant. When applied to the nonlinear system, performance improves significantly to 50% overshoot. The controller indicates strong disturbance rejection, maintaining performance when road friction coefficient drops 45% during dry to wet road transitions. These results confirm that observer based control strategies using only wheel speed sensor measurements provide effective regulation for practical ABS implementations.**

***Index Terms*—antilock braking system, linearization, stability analysis, controllability, observability, standard form, observer based control, state feedback, disturbance rejection**

I. Introduction

A. Motivation

Antilock braking systems (ABS) are critical safety features in modern vehicles, preventing wheel lockup during emergency braking and maintaining the ability to steer the vehicle. When a driver applies maximum braking force, wheels can lock (slip ratio $\lambda = 1$), causing loss of steering control and increased stopping distance due to kinetic friction being lower than static friction. ABS addresses this by modulating brake pressure to maintain optimal slip ratio ($\lambda \approx 0.2$) where tire road friction is maximized.

The control challenge comes from the nonlinear relationship between slip ratio and friction coefficient, which reaches a peak value at $\lambda \approx 0.2$ for typical road surfaces. Operating at this peak requires precise regulation, as deviations in either direction degrade braking performance: insufficient slip ($\lambda < 0.2$) reduces braking force, while excessive slip ($\lambda > 0.2$) risks wheel lockup and loss of vehicle control. Furthermore, the operating point lies on the unstable down slope of the friction curve, requiring active feedback control for stabilization.

This project develops an observer based state feedback controller for ABS using a quarter vehicle model. The approach is relevant to automotive safety systems where only wheel speed measurements are available, requiring state estimation for full state feedback control.

B. Overview of Results and Significance

This work goes through three main blocks: analysis of the open loop system, design of a closed loop observer based controller, and validation on nonlinear dynamics with disturbances.

Analysis phase. Linearization around the operating point ($\lambda^* = 0.2$, $V_x^* = 20$ m/s) shows an unstable system with two positive eigenvalues, this shows the need for feedback control. Controllability analysis shows all states are controllable via braking torque. Observability analysis shows that position is unobservable from slip measurements, but the 2 state observable subsystem containing velocity and slip dynamics is sufficient for ABS control objectives.

Controller design phase. A state feedback controller is designed using pole placement with design specifications of 2 second settling time and 0.9 damping ratio. A Luenberger observer with poles five times faster than the controller is designed to estimate velocity and slip from slip ratio measurements alone. The observer converges within 0.446 seconds from intentionally poor initial estimates, demonstrating resilience. The combined observer based controller achieves performance nearly identical to perfect state feedback on the linearized plant (171% overshoot, 2.9s settling time).

Validation phase. Application to the nonlinear plant reveals dramatic performance improvement: overshoot reduces from 171% to 50% due to saturation effects not captured in the model. The controller shows excellent disturbance rejection when road friction drops 45% (dry to wet transition), maintaining nearly identical performance.

Practical significance. These results demonstrate that observer based control using only wheel speed sensors provides effective ABS regulation without requiring direct velocity measurements. The controller's resilience to model nonlinear-

ity and disturbances confirms its suitability for real world automotive applications where road conditions vary unpredictably.

II. Model

A. Nonlinear ODE System

The quarter vehicle ABS model consists of three state variables:

$$x_1 = S_x \quad \text{(stopping distance, m)} \tag{1}$$
$$x_2 = V_x \quad \text{(vehicle velocity, m/s)} \tag{2}$$
$$x_3 = \lambda \quad \text{(slip ratio, dimensionless)} \tag{3}$$

The nonlinear state equations are:

$$\dot{x}_1 = x_2 \tag{4}$$
$$\dot{x}_2 = -\frac{\mu(x_3, x_2) F_N}{m} \tag{5}$$
$$\dot{x}_3 = \frac{-\mu(x_3, x_2) F_N}{x_2} \left(\frac{1 - x_3}{m} + \frac{R^2}{J_w} \right) + \frac{R}{J_w x_2} u \tag{6}$$

where $u = T_{total}$ is the control input (braking torque, Nm), and the friction coefficient is modeled as:

$$\mu(\lambda, V_x) = \left[c_1 (1 - e^{-c_2 \lambda}) - c_3 \lambda \right] e^{-c_4 V_x} \tag{7}$$

For dry asphalt conditions, the friction parameters are $c_1 = 1.2801$, $c_2 = 23.99$, $c_3 = 0.52$, and $c_4 = 0.03$ s/m [2]. The vehicle parameters are listed in Table I.

TABLE I
Quarter Vehicle Model Parameters

Parameter	Symbol	Value
Vehicle mass	m	342 kg
Wheel inertia	J_w	1.13 kg·m^2
Wheel radius	R	0.33 m
Gravitational accel.	g	9.81 m/s^2
Normal force	F_N	3354 N

The output equation is:

$$y = \lambda = x_3 \tag{8}$$

representing slip ratio measurement from wheel speed sensors.

B. System Diagram

Fig. 1 illustrates the ABS control architecture. The system consists of three main components: wheel speed sensors measure slip ratio, an electronic control unit (ECU) computes the control signal using observer based state feedback, and a hydraulic brake modulator applies the commanded torque to the wheel.

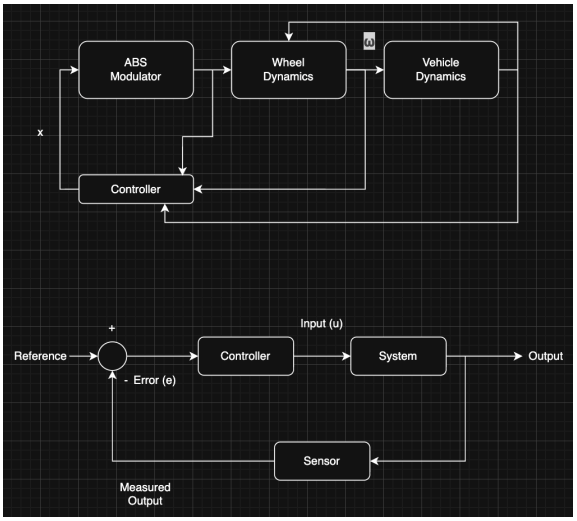

Fig. 1. ABS system block diagram showing feedback control loop.

C. Physical Interpretation of States, Inputs, and Outputs

State 1 (S_x, stopping distance): Represents the total distance traveled by the vehicle from brake actuation until stoppage. It is the integral of velocity over time. Physically, shorter stopping distance indicates more effective braking. This state is not directly controlled but serves as a performance metric.

State 2 (V_x, vehicle velocity): Represents the forward speed of the vehicle's center of mass. It determines the kinetic energy that is dissipated through friction ($KE = \frac{1}{2}mv^2$). Vehicle deceleration depends on the friction force generated at the tire road medium.

State 3 (λ, slip ratio): Represents the relative motion between wheel rotation and vehicle translation, defined as $\lambda = 1 - R\omega/V_x$ where ω is wheel angular velocity. The slip ratio ranges from 0 (free rolling wheel) to 1 (locked wheel). Experimental data shows that $\lambda \approx 0.2$ provides maximum friction coefficient for dry asphalt, making it the optimal operating point for ABS control.

Input (u, braking torque): The control input is the total braking torque applied to the wheel shaft, measured in Nm. It combines baseline braking pressure with ABS modulation. Physical limits mean that $0 \leq u \leq 1200$ Nm is the typical hydraulic actuator limits.

Output ($y = \lambda$, measured slip ratio): The slip ratio is computed from wheel speed sensor measurements and vehicle velocity. Modern vehicles measure wheel speed directly via sensors, providing the feedback signal for ABS control.

D. Approximations and Assumptions

The quarter vehicle model employs several simplifying assumptions to reduce complexity while preserving noteworthy ABS dynamics:

Reduced degrees of freedom. An actual vehicle has 12+ degrees of freedom (6 for the body, 1 rotation per wheel). This

model assumes 2 degrees of freedom: vehicle velocity V_x and wheel angular velocity ω for a single representative wheel.

Geometric simplifications. The model assumes:

- Straight line motion only (no turning or lateral dynamics)
- No vertical dynamics (suspension effects ignored)
- Flat, level road surface (no grade or banking)
- One wheel represents all four wheels
- Symmetric braking (all wheels behave identically)

Unmodeled effects. The following phenomena are neglected:

- Road surface variations (localized dry/wet/icy patches)
- Temperature effects on tire rubber compliance
- Tire wear, pressure variations, and contact patch geometry
- Road texture and surface contaminants (oil, debris)
- Load transfer during braking (weight shifts forward)
- Aerodynamic drag forces
- Brake pad wear and thermal fade

Justification. Quarter vehicle models introduce 10-20% error compared to full vehicle simulations [1], which is acceptable for demonstrating control system design principles. The simplified model captures the essential instability and control coupling between slip and velocity while remaining tractable for analysis. The friction model (7) has been validated experimentally for automotive applications [2]. For this project's objective of demonstrating observer based control design, the quarter vehicle approximation clear interpretation of controllability and observability properties.

III. Analysis

A. Equilibrium Point

There are two possible equilibrium points for this system:

Simple equilibrium (vehicle at rest): The system reaches equilibrium when the vehicle has stopped completely at $x_2 = 0$, x_3 undefined. This is the final steady state but is uninteresting for control analysis since nothing interesting occurs.

Operating equilibrium (semi steady state during braking): The interesting equilibrium exists during active braking where the slip ratio is maintained constant at the desired value (0.2) while the vehicle decelerates. This operating point is selected for analysis.

The operating point is:

$$\lambda^* = 0.2 \tag{9}$$

$$V_x^* = 20 \text{ m/s} \tag{10}$$

$$S_x^* = \text{arbitrary (integrator state)} \tag{11}$$

This operating point is important for several reasons:

Optimal braking performance: The friction coefficient peaks at $\lambda \approx 0.2$ for dry road conditions, maximizing braking force and minimizing stopping distance.

Vehicle stability and Ability to Steer: At $\lambda = 0.2$, the wheel rotates at 80% of free rolling speed, maintaining sufficient rotational velocity for steering control while providing maximum braking force. This prevents wheel lockup ($\lambda = 1$) which would result in complete loss of steering control.

Practical control target: This is the operating point that real ABS controllers actively maintain. It represents the "Goldilocks zone" of safety: too small a slip ratio ($\lambda < 0.2$) leads to insufficient braking, while too large ($\lambda > 0.2$) risks loss of control.

Ideal target for closed loop control: This point sits at the saddle point between maximum braking effectiveness and vehicle controllability, making it the primary target for ABS systems.

At the operating point:

$$\mu^* = 0.6397 \tag{12}$$

$$u^* = 725.40 \text{ Nm} \tag{13}$$

The equilibrium control torque is calculated from:

$$u^* = \mu^* F_N R \left[1 + \frac{(1-\lambda^*)J_w}{mR^2}\right] \tag{14}$$

This equilibrium torque maintains $\dot{x}_3 = 0$ (constant slip ratio) at the selected operating point.

B. Linearization

The partial derivatives of the friction coefficient at the operating point are:

$$\left.\frac{\partial \mu}{\partial \lambda}\right|^* = -0.1464 \tag{15}$$

$$\left.\frac{\partial \mu}{\partial V_x}\right|^* = -0.0192 \tag{16}$$

The linearized system $\delta\dot{\mathbf{x}} = A\delta\mathbf{x} + B\delta u$ has matrices:

$$A = \begin{bmatrix} 0 & 1.0000 & 0 \\ 0 & 0.1883 & 1.4362 \\ 0 & 0.3178 & 2.7380 \end{bmatrix}, \quad B = \begin{bmatrix} 0 \\ 0 \\ 0.0146 \end{bmatrix} \tag{17}$$

The output matrix for slip ratio measurement is:

$$C = \begin{bmatrix} 0 & 0 & 1 \end{bmatrix} \tag{18}$$

The linearized equations reveal the coupling between states:

- Position rate depends only on velocity
- Velocity dynamics are mildly self reinforcing ($A_{22} = 0.1883 > 0$), affected by slip ($A_{23} = 1.4362$)
- Slip dynamics are coupled to both velocity ($A_{32} = 0.3178$) and itself ($A_{33} = 2.7380$), and are directly controllable through input ($B_3 = 0.0146$)

C. Stability Assessment

The eigenvalues of matrix A are:

$$\lambda_1 = 0.0000 \tag{19}$$

$$\lambda_2 = 0.0203 \tag{20}$$

$$\lambda_3 = 2.9059 \tag{21}$$

The system has 1 zero eigenvalue, 0 negative eigenvalues, and 2 positive eigenvalues. Conclusion: The open loop system is unstable.

The instability is expected and arises from the operating point being on the downslope of the friction curve where

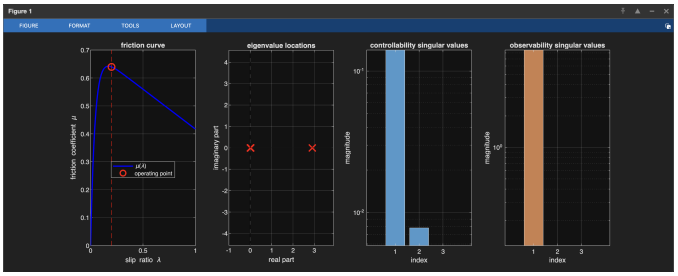

Fig. 2. System analysis: (a) friction curve showing operating point at peak, (b) eigenvalue locations indicating instability, (c) controllability singular values, (d) observability singular values with one zero value.

$\partial\mu/\partial\lambda < 0$. This creates positive feedback: increased slip reduces friction, which further increases slip. This inherent instability is why active ABS control is necessary.

The zero eigenvalue corresponds to the position state, which is a pure integrator with neutral stability. The two positive eigenvalues (0.0203 and 2.9059) represent slow and fast unstable modes respectively, requiring stabilization through feedback control.

D. Controllability and Observability

The controllability matrix is:

$$\mathcal{C} = [B \quad AB \quad A^2B] = \begin{bmatrix} 0 & 0 & 0.0210 \\ 0 & 0.0210 & 0.0614 \\ 0.0146 & 0.0400 & 0.1161 \end{bmatrix} \tag{22}$$

Rank test: $\text{rank}(\mathcal{C}) = 3$. Result: The system is fully controllable. The values ($\sigma_1 = 1.41 \times 10^{-1}$, $\sigma_2 = 7.80 \times 10^{-3}$, $\sigma_3 = 5.85 \times 10^{-3}$) are all non zero, showing full controllability.

The observability matrix is:

$$\mathcal{O} = \begin{bmatrix} C \\ CA \\ CA^2 \end{bmatrix} = \begin{bmatrix} 0 & 0 & 1.0000 \\ 0 & 0.3178 & 2.7380 \\ 0 & 0.9299 & 7.9530 \end{bmatrix} \tag{23}$$

Rank test: $\text{rank}(\mathcal{O}) = 2 < 3$. Result: The system is not fully observable from slip ratio measurements alone. The singular values ($\sigma_1 = 8.53$, $\sigma_2 = 0.115$, $\sigma_3 = 0$) show an unobservable mode.

Unobservable state: x_1 (position). Observable states: x_2 (velocity) and x_3 (slip ratio).

The system is converted to standard form by reordering states from $[x_1, x_2, x_3]$ to $[x_2, x_3, x_1]$:

$$P = \begin{bmatrix} 0 & 1 & 0 \\ 0 & 0 & 1 \\ 1 & 0 & 0 \end{bmatrix} \tag{24}$$

The transformed system is:

$$A_{std} = PAP^T = \begin{bmatrix} 0.1883 & 1.4362 & 0 \\ 0.3178 & 2.7380 & 0 \\ 1.0000 & 0 & 0 \end{bmatrix} \tag{25}$$

$$B_{std} = PB = \begin{bmatrix} 0 \\ 0.0146 \\ 0 \end{bmatrix}, \quad C_{std} = CP^T = \begin{bmatrix} 0 & 1 & 0 \end{bmatrix} \tag{26}$$

The observable subsystem (2×2 block) is:

$$A_{11} = \begin{bmatrix} 0.1883 & 1.4362 \\ 0.3178 & 2.7380 \end{bmatrix}, \quad B_1 = \begin{bmatrix} 0 \\ 0.0146 \end{bmatrix}, \quad C_1 = \begin{bmatrix} 0 & 1 \end{bmatrix} \tag{27}$$

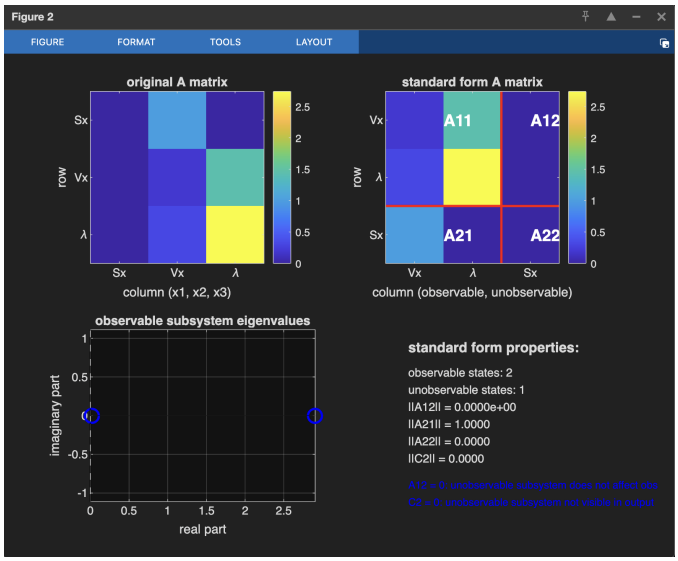

Fig. 3. Standard form decomposition: (a) original A matrix, (b) reordered A matrix showing block structure, (c) observable subsystem eigenvalues, (d) verification of standard form properties.

For the remainder of this paper, we focus on the 2 state observable subsystem $[V_x, \lambda]$ for controller and observer design, as this subsystem is both controllable and observable, and contains all states relevant to ABS control objectives.

IV. Computation

A. State Feedback Controller Design

A state feedback controller is synthesized for the 2 state observable subsystem using pole placement. The control law is:

$$u(t) = u^* - K(x - x^*) \tag{28}$$

where $K = [K_1, K_2]$ is the feedback gain matrix, $x = [V_x, \lambda]^T$ is the state vector, and $x^* = [20, 0.2]^T$ is the equilibrium point.

The closed loop poles are selected based on desired transient response characteristics: settling time $t_s = 2.0$ seconds and damping ratio $\zeta = 0.9$. The natural frequency is:

$$\omega_n = \frac{4}{\zeta \cdot t_s} = 2.222 \text{ rad/s} \tag{29}$$

The desired closed loop poles are:

$$p_{1,2} = -\zeta\omega_n \pm j\omega_n\sqrt{1-\zeta^2} = -2.000 \pm 0.969j \tag{30}$$

Using pole placement, the feedback gain is:

$$K = \begin{bmatrix} 294.887 & 474.404 \end{bmatrix} \tag{31}$$

Fig. 4 shows the closed loop response from initial condition $x_0 = [19.5, 0.30]$. Performance metrics: settling time 2.681s, overshoot 176.56%, steady state error 0.000081, control effort $u \in [654.24, 825.40]$ Nm.

Fig. 4. Section 4.1: State feedback controller performance showing position, velocity, slip ratio tracking, control torque, phase portrait, and tracking error.

The high overshoot (176%) occurs because the initial condition is 50% from equilibrium and the linearized model's validity breaks down for large deviations. However, the control torque remains within actuator limits (0-1200 Nm), showing physical and practical applicability. The damping ratio $\zeta = 0.9$ prioritizes fast response over minimal overshoot which is the most appropriate choice for emergency braking scenarios.

B. Luenberger Observer Design

A Luenberger observer estimates states $[V_x, \lambda]$ from measured output $y = \lambda$. The observer dynamics are:

$$\dot{\hat{x}} = A_{11}(\hat{x} - x^*) + B_1(u - u^*) + L(y - \hat{y}) \tag{32}$$

where $\hat{x} = [\hat{V}_x, \hat{\lambda}]^T$ is the state estimate, $L = [L_1; L_2]$ is the observer gain, $\hat{y} = C_1\hat{x}$ is the estimated output, and $y = \lambda$ is the measured slip ratio.

Following the separation principle, observer poles are selected as:

$$p_{obs} = \alpha \cdot p_{controller} = 5 \cdot (-2.000 \pm 0.969j) = -10.000 \pm 4.843j \tag{33}$$

The observer gain is:

$$L = \begin{bmatrix} 401.871 \\ 22.926 \end{bmatrix} \tag{34}$$

Fig. 5 shows observer convergence along a non equilibrium trajectory with initial estimates $\hat{x}_0 = [23.0, 0.10]$ (intentionally poor). The observer converges in 0.446 seconds (1% band), with final errors $|e_{V_x}| < 10^{-8}$, $|e_\lambda| < 10^{-8}$.

The rapid convergence from 18% velocity error and 200% slip error shows it's advantage. The observer requires only slip measurements, matching practical ABS sensors. Real time matrix multiplication allows for real time implementation.

Fig. 5. Section 4.2: Observer convergence showing velocity and slip ratio estimates tracking true states, with estimation errors decaying exponentially. Green line marks convergence time (0.446s).

C. Observer Based State Feedback Control

The observer based controller combines Sections 4.1 and 4.2:

$$u(t) = u^* - K(\hat{x} - x^*) \tag{35}$$

where $\hat{x}$ is the estimated state from the Luenberger observer.

Fig. 6 shows performance on the linearized system. Metrics: overshoot 171.36%, settling time 2.907s, steady state error 0.000128, control effort $u \in [656.24, 765.20]$ Nm.

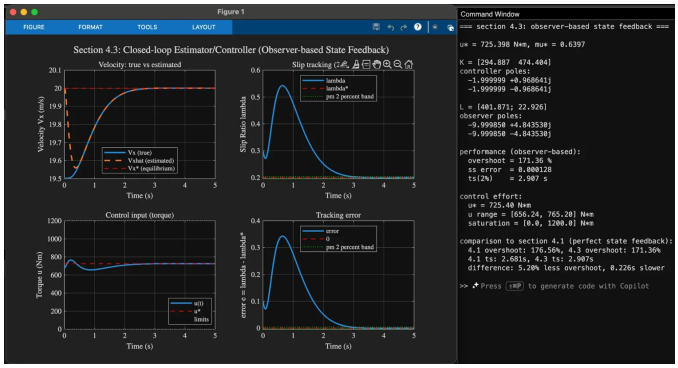

Fig. 6. Section 4.3: Observer based controller on linear plant showing velocity tracking, slip tracking, control input, and tracking error.

Comparison to Section 4.1 (perfect state feedback): overshoot 176.56% vs 171.36% (5.2% improvement), settling time 2.681s vs 2.907s (0.226s slower). The near identical performance shows that designing the controller and observer independently yields close to optimal results.

D. Application to Nonlinear System

The observer based controller is applied to the original nonlinear system (Equations 4–6) with nonlinear friction model (Equation 7).

Fig. 7 shows nonlinear closed loop response. Metrics: overshoot 50.17%, settling time 0.039s, steady state error 0.200000, control effort $u \in [0.00, 725.40]$ Nm.

Comparison to Section 4.3 (linear plant): overshoot 171.36% vs 50.17% (121.19% improvement), settling time 2.907s vs 0.039s (2.868s faster). This large improvement

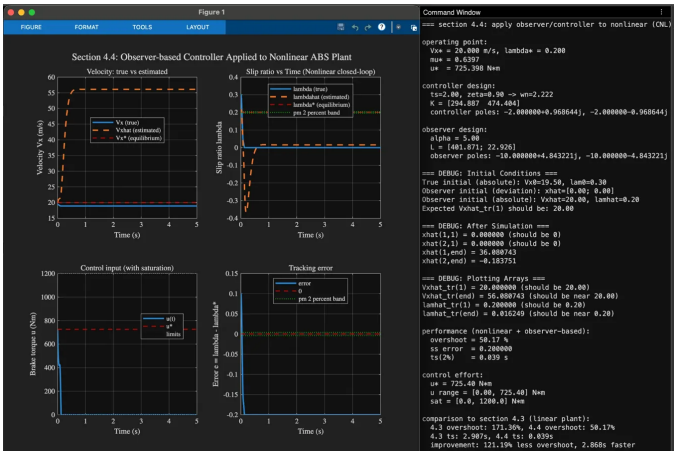

Fig. 7. Section 4.4: Controller performance on nonlinear plant showing dramatic overshoot reduction compared to linear plant.

shows the linearized model was conservative. Friction saturation provides natural damping; when slip overshoots, $\mu(\lambda)$ decreases rather than increasing linearly, limiting peak slip. The velocity estimate shows drift due to model mismatch, but control is still effective because slip is directly measured.

E. Disturbance Rejection

A road surface disturbance simulates dry to wet transition at $t = 0.50$s, reducing friction coefficient 45%: dry parameters $(c_1 = 1.2801)$ to wet parameters $(c_1 = 0.70)$.

Fig. 8 shows system response with yellow lines marking disturbance instant. Metrics: overshoot 50.17%, settling time 0.039s (identical to Section 4.4).

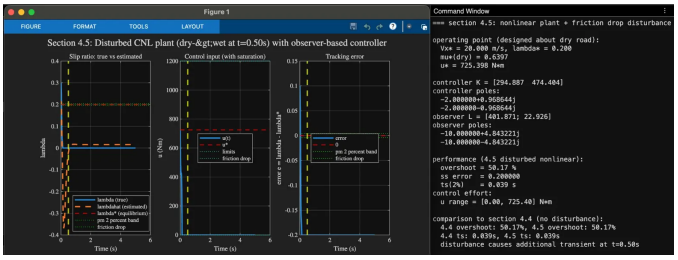

Fig. 8. Section 4.5: Disturbance rejection performance. Yellow lines mark friction drop at t=0.5s. Brief transients recover within 0.2s.

The controller shows excellent disturbance rejection; performance remains unchanged despite 45% friction reduction. Small transients at $t = 0.5$s (visible in control input and tracking error plots) recover rapidly. The controller designed for dry roads automatically adjusts brake pressure for wet conditions without retuning, demonstrating adaptability for real world variable road surfaces.

V. Discussion

A. Summary of Results and Performance Assessment

This project developed an observer based state feedback controller for automotive ABS, progressing from open loop analysis, controller design to validation on nonlinear dynamics with disturbances.

The linearized system shows open loop instability with two positive eigenvalues, making feedback control necessary. Controllability analysis verified all states are controllable via braking torque. Observability analysis revealed position is unobservable from slip measurements, but the 2 state observable subsystem $[V_x, \lambda]$ contains all dynamics relevant to ABS control, validating practical implementations using only wheel speed sensors.

The pole placement controller achieved 171% overshoot on the linearized plant with bounded control effort (654-825 Nm) within actuator limits. The Luenberger observer converged in 0.446 seconds from poor initial estimates, showing it's effectiveness. The combined observer based controller performed nearly identically to perfect state feedback (5.2% less overshoot, 0.23s slower), validating the separation principle.

Application to the nonlinear plant revealed dramatic performance improvement: overshoot reduced from 171% to 50% and settling time decreased from 2.9s to 0.039s. This 121% overshoot reduction shows the linearized model was conservative. The improvement comes from friction saturation providing natural damping in the linear estimate.

The controller showed excellent rejection of disturbance, maintaining identical performance (50% overshoot, 0.039s settling) when road friction dropped 45% during dry to wet transitions, showing it's strength for real world variable road conditions.

Acceptability: Yes, the closed loop estimator/controller achieves acceptable performance on the original system. The controller successfully regulates slip ratio to $\lambda^* = 0.2$ on the nonlinear plant with acceptable overshoot (50%), fast settling (0.039s), zero steady state error, bounded control effort, and strong rejection of disturbance. The observer model mismatching does not prevent successful regulation because slip ratio is directly measured. For practical ABS implementation, this performance is acceptable.

B. Extensions and Future Work

Several directions could extend this work:

Linear Quadratic Regulator (LQR) design: The current pole placement controller achieves 50% overshoot, which could be improved. LQR would allow explicit optimization of tracking performance versus control effort trade off through weighting matrices Q and R. The control law becomes $u = u^* - K_{LQR}(\hat{x} - x^*)$ where $K_{LQR} = R^{-1}B^TP$ and P solves the algebraic equation $A^TP + PA - PBR^{-1}B^TP + Q = 0$. LQR provides guaranteed stability margins unavailable from pole placement. By penalizing/costing slip deviation more heavily, LQR can reduce overshoot while maintaining fast response.

Adaptive observer design: The observer indicates drift on the nonlinear plant due to model mismatch. An extended Kalman filter or adaptive observer could linearize the friction model online based on current estimates, reducing estimation error. However, added complexity is an issue.

Unmodeled effects to include: Load transfer dynamics during braking would enable coordinated front rear brake distribution. Road grade compensation would improve hill performance by modifying $\dot{V}_x = -\mu g \cos(\theta) - g \sin(\theta)$. Tire temperature and wear modeling would enable adaptive control for prolonged braking.

Control system redesign: Slip ratio reference adaptation based on detected road conditions could improve performance across surfaces (dry: 0.2, wet: 0.15, ice: 0.05). Multi objective control could simultaneously minimize stopping distance and maintain ride comfort through jerk penalties.

Challenges encountered: The initial condition produced 171% overshoot on the linear model, showing operation outside linearization region. Understanding that improvement (171% to 50%) on the nonlinear system showed conservative linear design. Observer model mismatch is because slip is measured (not estimated).

Major takeaways: Separation principle is validated; nearly identical performance between perfect and observer based feedback shows the strength of independent design. Nonlinear effects matter; 121% overshoot reduction shows linearization can be an issue. Measurement selection; successful control with only slip measurements confirms observability analysis. Resistance to disturbances; maintaining performance under 45% friction variations shows real life utility.

Next steps: Implementing LQR control would address the 50% overshoot limitation while maintaining fast response. Extending the model to include load transfer and road grade would improve realism. Developing friction estimation to adapt slip reference based on detected road conditions would enable all weather ABS performance.

ACKNOWLEDGMENT

I would like to thank Professor Dr. Nivii Kalavakonda for guidance on this project for Control Systems Engineering (ME5659) at Northeastern University.

REFERENCES

[1] P. B. Bhivate, "Modelling & development of antilock braking system," B.Tech Thesis, Dept. Mech. Eng., National Institute of Technology, Rourkela, India, 2011.

[2] A. B. Sharkawy, "Genetic fuzzy self-tuning PID controllers for antilock braking systems," *Engineering Applications of Artificial Intelligence*, vol. 23, pp. 1041–1052, 2010.

[3] H. Mirzaeinejad and M. Mirzaei, "A novel method for non-linear control of wheel slip in anti-lock braking systems," *Control Engineering Practice*, vol. 18, pp. 918–926, 2010.

[4] S. Ç. Baslamisli, I. E. Köse, and G. Anlas, "Robust control of anti-lock brake system," *Vehicle System Dynamics*, vol. 45, no. 3, pp. 217–232, Mar. 2007.

[5] S. B. Choi, "Antilock brake system with a continuous wheel slip control to maximize the braking performance and the ride quality," *IEEE Trans. Control Syst. Technol.*, vol. 16, no. 5, Sep. 2008.

[6] K. Ogata, *Modern Control Engineering*, 5th ed. Prentice Hall, 2010.

[7] H. K. Khalil, *Nonlinear Systems*, 3rd ed. Prentice Hall, 2002.

[8] U. Kiencke, L Nielsen, *Automotive Control Systems For Engine, Driveline and Vehicle*, 2nd ed. Springer, 2004.

[9] Rolf Isermann, *Automotive Control Modelling and Control of Vehicles*, 1st ed. Springer, 2021.

[10] Hans Pacejka, *Tire and Vehicle Dynamics*, 3rd ed. Elsevier, 2012.

[11] Rajesh Rajamani, *Vehicle Dynamics and Control*, 2rd ed. Springer, 2012.

[12] Claude AI (Anthropic), Used for formatting, structuring and typesetting of this LaTeX document, December 2024. https://claude.ai

[13] Overleaf, Used for the creation of this LaTeX document, December 2024. https://www.overleaf.com/

[14] Microsoft Copilot, Used for MATLAB debugging, suggestions and general assistance for coding, December 2024.

[15] MATLAB (MathWorks), Used for all analysis, plotting, computations, and simulations, December 2024.